Synthesis and characterterization of nanostructured CeO_2 by solvothermal method and its energy application

Yashodeo Mishra & Susanta Sinha Mahapatra*
Department of Chemistry, Birla Institute of Technology, Mesra, Ranchi 835215, Jharkhand, India

DOI: 10.3578/jecsi.68.3&4.2019.79

Abstract:

The Highly ordered octahedral CeO_2 nanoparticles were synthesized solvothermally. CeO_2 nanoparticles were deposited on the chemically etched Si Nanowires and the electrode was used as anodic material for supercapacitors. The structure and morphologies of sample prepared were characterized by X-Ray Diffraction, Field Emission Scanning Electron Microscope. The electrochemical tests were performed using three-electrode work station which exhibits superior electrochemical performance including high specific capacitance and good cycling stability. The electrochemical property is attributed to the redox nature due to which ceria shows good physicochemical properties along with chemical and mechanical stability. Owing to the ease of good electrochemical properties and large scale fabrication, these CeO_2/Si-NWs array would be promising anode material for supercapacitors. The assembled CeO_2/Si-NWs anode exhibited excellent electrochemical specific capacitance of 846 Fg^{-1}

Keywords: CeO_2 nanoparticles, Supercapacitors, CeO_2/Si-NWs, Solvothermal

1. Introduction

Supercapacitors have allured the researchers due to their multiple advantages such as high power density, outstanding cyclic behaviour, superior rate capability, relatively high energy density, rapid charging/discharging rate, broad operating temperature window. [1] Supercapacitors are mainly categorized into two types on the basis of charge storage mechanism: electrical double-layer capacitors (EDLCs), where energy storage is controlled by diffusion and accumulation of electrostatic charge at electrode and electrolyte interface; where as in pseudocapacitors faradaic redox reactions results in charge storage and consequently shows high specific capacitance. [1]

In recent years great enhancement is observed in the development of positive electrode materials in comparison to negative electrode materials which is somewhat slow.[2, 3] Metal oxides are promising candidates for the anode materials as they evince superior specific capacitance during the charging/discharging process by rapid and reversible Faradaic reactions.[4] With the advancement in the designing of electrode materials the materials which are environment friendly, abundant, excellent electrochemical redox behaviour are considered promising candidates for the electrode materials. CeO_2 displays exceptional redox behaviour and environment friendliness which presents it as a promising candidate for anode electrode material. [5] Rapid conversion of Ce(III) and Ce(IV), enables fast transfer of electrons and diffusion of Cerium ions.[6] However, the major challenge for its application as supercapacitor electrode is its low conductivity and ease of agglomeration. This drawback can be dealt by depositing them on highly conductive substrate.

One of the favourable substrate for its application as an energy storage device is Silicon. It is a suitable substrate as it is low-cost material, least toxic, and fabrication process is well known for Si-based materials [7-11]. It also possess an exceptional thermal, electronic and mechanical properties. The performance of the supercapictors is dependent upon the active surface area as the

contact area of the electrode electrolyte interface is directly proportional to energy storage[12]. Hochbaum et al.,[13] reported that non-porous silicon nanowires have significantly less surface area of ~ 24 m^2g^{-1} in comparison to the porous silicon nanowires synthesized by metal assisted chemical etching (MACE) having surface area of ~324 m^2g^{-1}.

Moreover, the advantage of using silicon nanowire over other silicon-based substrate is, it acts as current collector because the nanowires are etched into the silicon wafer and thus reduces the contact-resistance [14].

In this investigation, we fabricated highly ordered CeO_2/Si-NWs for efficient energy storage by hydrothermal deposition of CeO_2 upon Si-NWs which were synthesized by metal-assisted anodic chemical etching. The Fabricated electrode exhibited specific capacitance of 846 Fg^{-1} upon galvanostatic charge-discharge cycles at 5 Ag^{-1} in aqueous KOH electrolyte. The CeO_2/Si-NWs electrode delivers excellent electrochemical performance including high specific capacitance and good cycling stability.

Experimental

Materials and Methods

All the reagents were purchased from Sigma Aldrich of analytical grade and were used without any further purification in the experiments.

Synthesis of Si-Nanowires

Highly-doped single side polished n-type Si wafer (0.001S 0.005 Ù.cm) were used to synthesize highly ordered Si-NWs S 25 ìm in by metal assisted wet chemical etching [15]. Si-wafers (100) were cut into 10 mm^2 pieces, and were degreased ultrasonically in acetone and ethanol at ambient temperature for 10 minutes each. The pieces of wafer were then rinsed off in deionised water and immersed into 5% HF (V/V) solution for 1 min. Ag particles were then coated onto the wafer pieces by a dropping the wafers into the solution of 10% HF (V/V) and 0.02 M $AgNO_3$. The deposition of silver nanoparticles on the Silicon surface was inferred by the change in colour from shiny to colourful. The Ag-coated Si-wafers were rinsed off well in deionised water to remove excess Ag-particles and then placed into the etching solution, i.e 10% HF (V/V) and 0.6% H_2O_2 (V/V). The Si-wafers were etched for 4 hours. The etched Si-NWs were then dipped into 15% HNO_3 solution followed by submerging in 5% HF for 2 min to remove SiO_X layer. To remove the metal contamination this process was repeated thrice.

Synthesis of CeO_2

0.5 mM of PPh_3 and 2.0 mM of $Ce(NO_3).6H_2O$ were ultrasonicated in milliQ water and to this mixture 2M NaOH was slowly added till pH reached S 8. The solution was then transferred to 100 mL capacity, Teflon-lined autoclave and treated at 180 ^{0}C for 16 hour. The autoclave was allowed to cool naturally to the room temperature. The product was washed with milliQ water and ethanol twice and kept for drying in vacuum oven at 80 ^{0}C for 8 hour. This product was calcined at 700 ^{0}C for 2 hours at the ramping rate of 3 ^{0}C min^{-1} to get a pale yellow powder of CeO_2.

Fabrication of CeO_2/Si-NWs electrode

Working electrode was fabricated by using previously etched Si-NWs as substrate which was of 1 x 1 cm^2. The synthesized CeO_2 nanoparticles was mixed with acetylene black and PVDF in the ratio 80:10:10 by weight and slurry was prepared by adding few drops of NMP. The slurry was then coated onto the Si-NWs and kept to dry in hot air oven for 4 hours.

Structural Characterization

The X-ray diffraction was performed by Rigaku D/max-2500V X-ray diffractometer using Cu Ká (ë=0.15418 nm) radiation. The morphological studies were carried out using Field emission scanning electron microscopy (FE-SEM) Zeiss Sigma 300 integrated with energy-dispersive X-ray spectroscopy EDAX-Ametek.

Electrochemical Studies

Electrochemical studies were performed on electrochemical workstation (Autolab 302N) by cyclic voltammetry (CV) within the potential

window of 0 to + 0.5 V, galvanostatic charge-discharge (GCD) was performed at the current densities i.e 1 Ag^{-1}, 2 Ag^{-1} and 5Ag^{-1} respectively. Electrochemical impedence spectroscopy (EIS) was carried out in the frequency range of 100 kHz to 0.1 Hz. 3M KOH was used as electrolyte in a typical three-electrode system to perform all electrochemical measurements. CeO_2/Si-NWs was used as working electrode, Ag/AgCl as reference electrode and Pt-electrode as counter electrode.

Results and discussions

The Si-NWs synthesized in this investigation was obtained by metal assisted wet chemical etching method [15]. Ag nanoparticles acted as the catalyst for anisotropically etching the Si-wafer in HF/ H_2O_2 solution. FESEM analysis of the synthesized Si-NWs shown in figure-1, unveiled highly dense nanowire forest with an average height of 35-40 µm for 4 hours etched wafers.

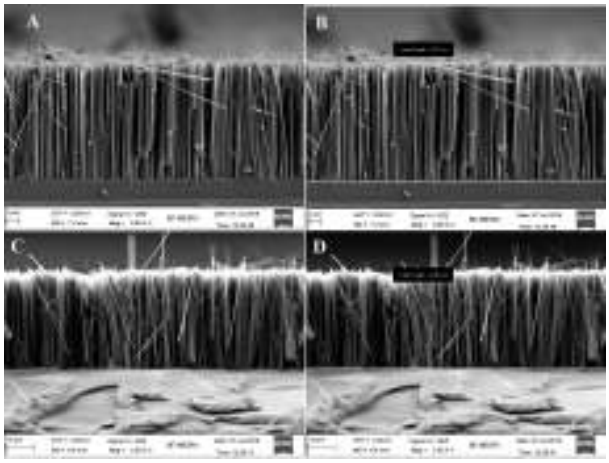


Figure 1. FESEM image of etched Si-NWs.

The crystallinity and phase purity of the CeO_2 was analysed using XRD technique as shown in figure-2. The intense peaks were observed at the 2è values of 28.30°, 32.95°, 47.50°, 56.39°, 58.90°,69.50° and 76.60° and can be indexed to (111), (200), (220), (311), (222), (400), (331), which matches well with the planes of cubic CeO_2 (JCPDS No.01-081-0792). This corresponds to the cubic structure of CeO_2 [16]. The morphological investigation was performed by FESEM, which suggests that the CeO_2 nanoparticles consisted of uniform octahedral as shown in figure-3. Signature peaks of Ce and O was observed in EDAX spectrum as seen in figure-4, thus displaying uniform distribution of elements Ce and O.

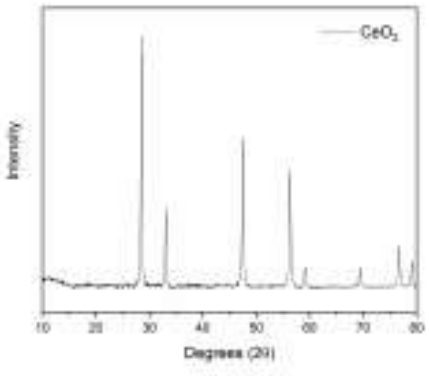


Figure 2. XRD pattern of CeO_2 nanoparticles



Figure 3. FESEM image of synthesized octahedral CeO_2

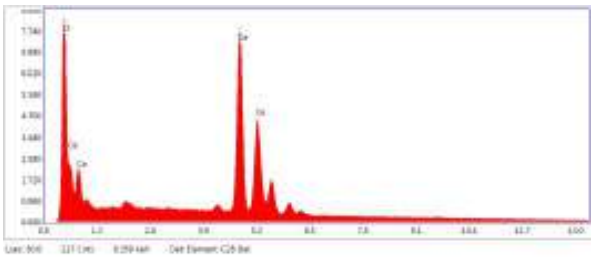


Figure 4 EDAX spectrum of CeO_2 nanopaticles

Table 1: Composition of the constituent elements in CeO_2

ELEMENT	WEIGHT (%)	ATOMIC(%)
O K	62.40	93.56
Ce L	37.60	6.44

CV of fabricated electrode was performed at different scan rates from 5mVs^{-1} to 50mVs^{-1} in the

potential window of 0.0V to 0.5V. The peaks in the curve (figure 5) represent oxidation half and reduction half, which signifies the redox behaviour of CeO_2 by showing the reversible conversion between Ce^{3+} and Ce^{4+} (equation 1) [17].

$$CeO_2 + e^- + H_2O \rightarrow Ce^{3+}OOH + OH^- \quad (1.a)$$

$$Ce^{3+}OOH^- + OH^- \rightarrow CeO_2 + OH^- + e^- \quad (1.b)$$

The CV curve of CeO_2/Si-NWs composite electrode principally retains faradaic peaks even at scan rates up to 50 mVs^{-1} which is symptomatic of a fast charge transport showing the behaviour of a pseudocapacitance. With the rise in scan rates, the magnitudes of the current and potential peak separation increase. Due to the polarization and ohmic resistance observed during the faradaic process, the oxidation and reduction peaks shift towards more positive and negative values respectively [18].

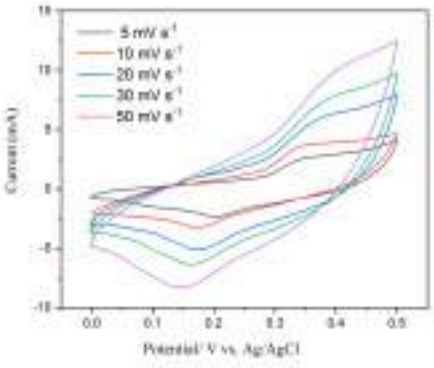


Figure 5. Cyclic voltametry of CeO_2/Si-NWs

GCD experiment was performed to study the effect of current density on specific capacitance. It was performed within potential window 0.0V to 0.5V in the varying current densities (1 Ag^{-1}, 2 Ag^{-1} and 5 Ag^{-1}) as shown in figure 6. The increase in the discharging time represents the higher capacitance, which corresponds to the result obtained in CV. Specific capacitance of the electrodes was calculated from the discharge curve according to the equation 2 where I = 1.41 x 10^{-3}, m = 0.40 mg, ΔV= 0.5 V, t =120 s and the result obtained was 846 Fg^{-1} at a current density of 1Ag^{-1} [16]. A little iR drop at the starting of every discharge curves is seen due to the presence of internal resistance [18].

$$C_s = \frac{I * \Delta t}{m * \Delta v} \quad (2)$$

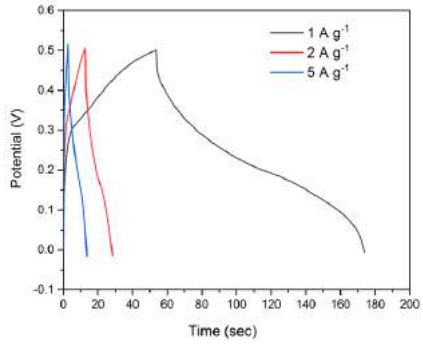


Figure 6. GCD plot of fabricated CeO_2/Si-NWs anode

EIS is performed to clarify the electrochemical characteristics of the ceria. It is a powerful technique to examine the kinetics during the electrochemical process. EIS test can reflect internal resistance of electrode material as shown by the Nyquist plot (figure 7). Tests were performed in a 3M KOH in the frequency range of 0.1Hz-100kHz [17]. A semicircle observed in the high frequency region is due to the charge transfer resistance (R_{CT}) which is associated with the faradaic reactions. The electrolyte resistance and the contact resistance between the current collector and the active material together form the equivalent series resistance (R_S). The intrinsic resistance of the electro-active material is evaluated from the high frequency of the impedance curve. The fitted equivalent circuit diagram of the Nyquist plot is shown in the inset of figure 7. The double layer capacitance formed at the junction of the electrolyte and electroactive material is represented as the constant phase element (CPE). R_L represents the leakage resistance during the electrochemical activities whereas the impedance because of the diffusion of the OH^- ions within the pores of CeO_2/SiNW electrode is represented by Warburg element (W). From the plot before cycling stability test, in the low frequency region, the impedance reflects the capacitive behaviour [18].

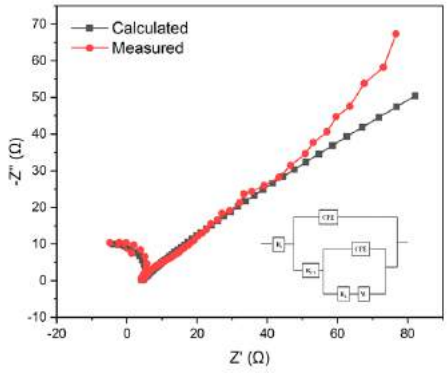


Figure 7. Nyquist plot of CeO_2/Si-NWs

Conclusion

A facile solvothermal/hydrothermal method is successfully synthesize octahedral CeO_2 particles obtained were anchored on the Si-NWs using chemical methods. The CeO_2/Si-NWs electrode has shown the higher specific capacitance and demonstrated an enhanced capacitive performance in terms of specific capacitance 846 Fg^{-1} in comparison to some other carbon based CeO_2 hybrids (Table 2). The assembled device displays excellent supercapacitve performance with mechanical and electrochemical stability. Such rationally designed supercapacitor proves to be a suitable candidate as the electrode material and promising pathway for the development of flexible energy storage devices with high performance to drive stretchable and wearable electronic devices for the future advanced applications.

Acknowledgement

We are thankful to Board of Research in Nuclear Sciences (BRNS), Government of India (Sanction No 34/14/2016-BRNS/34366) for financial assistance and Central Instrumentation Facility (CIF), BIT, esra for their analytical support.

Table 2: Comparative study of capacitance of CeO_2 hybrids

MATERIALS	CAPACITANCE (Fg^{-1})	CURRENT DENSITY(Ag^{-1}) OR SCAN RATE (mVs^{-1})	ELECTROLYTE USED	REFERENCE
CeO_2 /MWCNT	221.71	$2Ag^{-1}$	6 M KOH	[19]
CeO_2/ GO composite	382.94	$2Ag^{-1}$	6 M KOH	[20]
Graphene/CeO_2 aerogel composite	47.6	$1Ag^{-1}$	6 M KOH	[21]
Graphene/CeO_2 composite	109	$10mVs^{-1}$	1 M H_2SO_4	[22]
CeO_2/rGO composite	282	$2Ag^{-1}$	3 M KOH	[16]
CeO_2/CNT hybrid	818	$1mVs^{-1}$	2 M KOH	[17]
CNT/CeO_2 composite	289	$5mVs^{-1}$	0.5 Na_2SO_4	[23]
CeO_2 nanostructures	134	$1Ag^{-1}$	1 M KOH	[24]
CeO_2/Si-NWs hybrid	846	$1Ag^{-1}$	6 M KOH	This Work

References

1. Halper, M.S. and J.C. Ellenbogen, *Supercapacitors: A brief overview.* The MITRE Corporation, McLean, Virginia, USA, 2006: p. 1-34.
2. Tang, Q., et al., *Enhancing the energy density of asymmetric stretchable supercapacitor based on wrinkled CNT@ MnO2 cathode and CNT@ polypyrrole anode.* ACS applied materials & interfaces, 2015. **7**(28): p. 15303-15313.
3. Yu, M., et al., *Recent progress in the development of anodes for asymmetric supercapacitors.* Journal of Materials Chemistry A, 2016. **4**(13): p. 4634-4658.
4. Wang, Y., Y. Song, and Y. Xia, *Electrochemical capacitors: mechanism, materials, systems, characterization and applications.* Chemical Society Reviews, 2016. **45**(21): p. 5925-5950.
5. Maiti, S., A. Pramanik, and S. Mahanty, *Extraordinarily high pseudocapacitance of metal organic framework derived nanostructured cerium oxide.* Chemical Communications, 2014. **50**(79): p. 11717-11720.
6. Saravanan, T., et al., *Facile synthesis of graphene-CeO 2 nanocomposites with enhanced electrochemical properties for supercapacitors.* Dalton Transactions, 2015. **44**(21): p. 9901-9908.
7. Alper, J.P., et al., *Selective ultrathin carbon sheath on porous silicon nanowires: materials for extremely high energy density planar micro-supercapacitors.* Nano letters, 2014. **14**(4): p. 1843-1847.
8. Aradilla, D., et al., *High performance of symmetric micro-supercapacitors based on silicon nanowires using N-methyl-N-propylpyrrolidinium bis (trifluoromethylsulfonyl) imide as electrolyte.* Nano Energy, 2014. **9**: p. 273-281.
9. Chan, C.K., et al., *High-performance lithium battery anodes using silicon nanowires.* Nature nanotechnology, 2008. **3**(1): p. 31.
10. Liu, C., et al., *Nanowire–bacteria hybrids for unassisted solar carbon dioxide fixation to value-added chemicals.* Nano letters, 2015. **15**(5): p. 3634-3639.
11. Zhang, T., et al., *High thermoelectric figure-of-merits from large-area porous silicon nanowire arrays.* Nano Energy, 2015. **13**: p. 433-441.
12. Lang, X., et al., *Nanoporous metal/oxide hybrid electrodes for electrochemical supercapacitors.* Nature nanotechnology, 2011. **6**(4): p. 232.
13. Hochbaum, A.I., et al., *Single crystalline mesoporous silicon nanowires.* Nano letters, 2009. **9**(10): p. 3550-3554.
14. McGraw, M., et al., *One-step solid-state in-situ thermal polymerization of silicon-PEDOT nanocomposites for the application in lithium-ion battery anodes.* Polymer, 2016. **99**: p. 488-495.
15. Tang, H., et al., *Carrier dynamics in Si nanowires fabricated by metal-assisted chemical etching.* Acs Nano, 2012. **6**(9): p. 7814-7819.
16. Li, T. and H. Liu, *A simple synthesis method of nanocrystals CeO2 modified rGO composites as electrode materials for supercapacitors with long time cycling stability.* Powder Technology, 2018. **327**: p. 275-281.
17. Luo, Y., et al., *CeO2/CNTs hybrid with high performance as electrode materials for supercapacitor.* Journal of Alloys and Compounds, 2017. **729**: p. 64-70.
18. Pandit, B., B.R. Sankapal, and P.M. Koinkar, *Novel chemical route for CeO 2/MWCNTs composite towards highly bendable solid-state supercapacitor device.* Scientific reports, 2019. **9**(1): p. 5892.

19. Vanitha, M., P. Cao, and N. Balasubramanian, *Ag nanocrystals anchored CeO2/graphene nanocomposite for enhanced supercapacitor applications*. Journal of Alloys and Compounds, 2015. **644**: p. 534-544.

20. Dezfuli, A.S., et al., *A high performance supercapacitor based on a ceria/graphene nanocomposite synthesized by a facile sonochemical method.* RSC Advances, 2015. **5**(57): p. 46050-46058.

21. Wang, Y., et al., *CeO 2 nanoparticles/ graphene nanocomposite-based high performance supercapacitor.* Dalton Transactions, 2011. **40**(24): p. 6388-6391.

22. Shahrokhian, S., R. Mohammadi, and E. Asadian, *One-step fabrication of electrochemically reduced graphene oxide/ nickel oxide composite for binder-free supercapacitors.* International Journal of Hydrogen Energy, 2016. **41**(39): p. 17496-17505.

23. Kalubarme, R.S., Y.-H. Kim, and C.-J. Park, *One step hydrothermal synthesis of a carbon nanotube/cerium oxide nanocomposite and its electrochemical properties*. Nanotechnology, 2013. **24**(36): p. 365401.

24. Prasanna, K., et al., *Highly porous CeO2 nanostructures prepared via combustion synthesis for supercapacitor applications.* Applied Surface Science, 2018. **449**: p. 454-460.